DrillBit

The Report is Generated by DrillBit Plagiarism Detection Software

Submission Information

Author Name	Nuri Ari Efiana
Title	Self-emulsifying drug delivery systems containing sulfate-based surfactants: Are they responsive to alkaline phosphatase?
Paper/Submission ID	2232321
Submitted by	nurshifa.fauziyah@staff.uad.ac.id
Submission Date	2024-08-15 12:33:13
Total Pages, Total Words	8, 6931
Document type	Article

Result Information

Similarity **16 %**

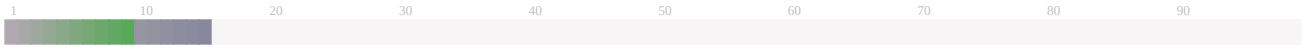

Sources Type

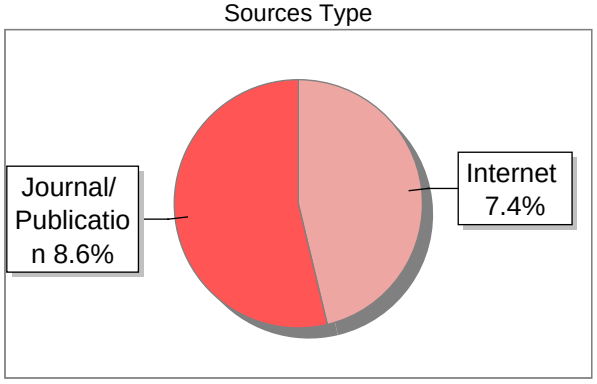

Report Content

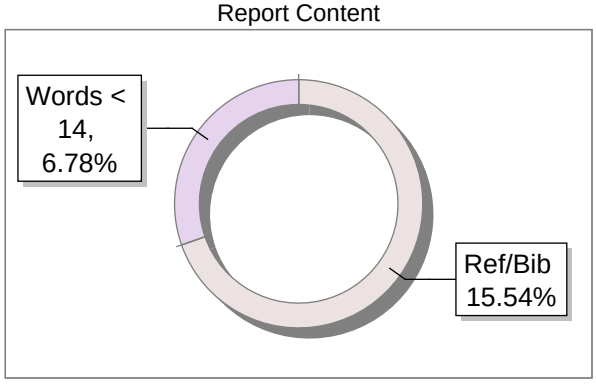

Exclude Information

Quotes	Excluded
References/Bibliography	Excluded
Source: Excluded < 14 Words	Not Excluded
Excluded Source	**17 %**
Excluded Phrases	Not Excluded

Database Selection

Language	English
Student Papers	Yes
Journals & publishers	Yes
Internet or Web	Yes
Institution Repository	Yes

A Unique QR Code use to View/Download/Share Pdf File

DrillBit

DrillBit Similarity Report

16	64	B
SIMILARITY %	MATCHED SOURCES	GRADE

A-Satisfactory (0-10%)
B-Upgrade (11-40%)
C-Poor (41-60%)
D-Unacceptable (61-100%)

LOCATION	MATCHED DOMAIN	%	SOURCE TYPE
3	biomedcentral.com	1	Internet Data
4	Formulation development of an albendazole self-emulsifying drug delivery system by -2012	1	Publication
5	bulletin.mfd.org.mk	1	Publication
6	bioresources.cnr.ncsu.edu	1	Internet Data
7	www.doaj.org	1	Publication
8	Site-Specific Trastuzumab Maytansinoid AntibodyDrug Conjugates with Improved Th by Pillow-2014	<1	Publication
9	An engineered lipocalin that tightly complexes the plant poison colchicine for u by Skerra-2018	<1	Publication
10	dovepress.com	<1	Internet Data
11	ECR plasma deposited a-SiCNH as insulating layer in piezoceramic modules by Peter-2018	<1	Publication
12	dovepress.com	<1	Internet Data
13	moam.info	<1	Internet Data
14	refubium.fu-berlin.de	<1	Publication

15	link.springer.com	<1	Internet Data
16	biomedcentral.com	<1	Internet Data
17	www.readbag.com	<1	Internet Data
19	Interaction of Ionic Surfactants with a Hydrophobic Modified Thermosen by Zhang-2014	<1	Publication
20	refubium.fu-berlin.de	<1	Publication
21	Thesis submitted to shodhganga - shodhganga.inflibnet.ac.in	<1	Publication
22	Thesis Submitted to Shodhganga Repository	<1	Publication
23	springeropen.com	<1	Internet Data
24	dovepress.com	<1	Internet Data
25	mdpi.com	<1	Internet Data
26	www.pnas.org	<1	Publication
27	High mobility n-channel organic field-effect transistors based on soluble C60 an by Pau-2008	<1	Publication
28	mdpi.com	<1	Internet Data
29	moam.info	<1	Internet Data
30	springeropen.com	<1	Internet Data
31	Thesis Submitted to Shodhganga Repository	<1	Publication
32	Promising Performance of 4HMS, a New Zirconium-89 Octadendate Chelator by Alnahwi-2020	<1	Publication
33	The potential of gibberellic acid 3 (GA3) and Tween-80 induced phytoremediation by Sun-2013	<1	Publication

34	www.intechopen.com	<1	Publication
35	www.mdpi.com	<1	Internet Data
36	centaur.reading.ac.uk	<1	Publication
37	downloads.hindawi.com	<1	Publication
38	eprints.covenantuniversity.edu.ng	<1	Publication
39	Intra- and interobserver reliability and intra-catheter reproducibili, by Antonsen, Lisbeth - 2015	<1	Publication
40	pdfcookie.com	<1	Internet Data
41	Preparation of a hordein-quercetin-chitosan antioxidant electrospun nanofibre fi by Li-2020	<1	Publication
42	vsijournal.org	<1	Internet Data
43	academicjournals.org	<1	Publication
44	bi.tbzmed.ac.ir	<1	Publication
45	Degradation of normetanephrine and norparanephrine in human blood by Jean-Mari-1971	<1	Publication
46	dovepress.com	<1	Internet Data
47	Electrical coupling underlies theta oscillations recorded in hippocam, by Jan Konopacki Toma- 2004	<1	Publication
48	Evaluation of biodegradability on polyaspartamide-polylactic acid based nanopart by Craparo-2015	<1	Publication
49	Introduction to time-of-flight secondary ion mass spectrometry applic, by Andrej Orik Hein- 2005	<1	Publication

50	Ligand-mediated internalization of glucagon receptors in intact rat liver by Authier-1992	<1	Publication
51	link.springer.com	<1	Internet Data
52	Main bioactive phenolic compounds in marine algae and their mechanisms of action by Jimenez-Lopez-2021	<1	Publication
53	moam.info	<1	Internet Data
54	moam.info	<1	Internet Data
55	moam.info	<1	Internet Data
56	nature.com	<1	Internet Data
57	Self-emulsifying drug delivery systems (SEDDS) The splendid comeback of an old by Bernkop-Schnrch-2019	<1	Publication
58	Smart Composite Sandwich Structures for Future Aerospace Application -Damage Det by TAKEDA-2007	<1	Publication
59	www.jove.com	<1	Internet Data
60	www.ncbi.nlm.nih.gov	<1	Internet Data
61	www.ncbi.nlm.nih.gov	<1	Internet Data
66	moam.info	1	Internet Data
72	Cadmium Induced p53-Dependent Activation of Stress Signaling, Accumula by Yu-2011	<1	Publication
86	Ligand-mediated internalization of glucagon receptors in intact rat liver by Authier-1992	1	Publication
90	Thesis submitted to shodhganga - shodhganga.inflibnet.ac.in	<1	Publication
95	springeropen.com	<1	Internet Data

116	www.banglajol.info	<1	Publication

EXCLUDED SOURCES

1	www.dx.doi.org	16	Publication
2	Lectin coupled liposomes for pulmonary delivery of salbutamol sulphate by Bonde-2019	2	Publication

Journal of Drug Delivery Science and Technology 96 (2024) 105717

Contents lists available at ScienceDirect

Journal of Drug Delivery Science and Technology

journal homepage: www.elsevier.com/locate/jddst

Self-emulsifying drug delivery systems containing sulfate-based surfactants: Are they responsive to alkaline phosphatase?

Ahmad Saleh [a,b], Zeynep Burcu Akkuş-Dağdeviren [a], Florina Veider [a], Nuri Ari Efiana [a,c], Andreas Bernkop-Schnürch [a,*]

[a] Center for Chemistry and Biomedicine, Department of Pharmaceutical Technology, Institute of Pharmacy, University of Innsbruck, Innrain 80/82, 6020, Innsbruck, Austria

[b] Department of Pharmacy, Universitas Mandala Waluya, A.H.Nasution, Kendari, 93231, Southeast Sulawesi, Indonesia

[c] Department of Pharmaceutical Technology, Faculty of Pharmacy, Universitas Ahmad Dahlan, Jl. Prof. Dr. Soepomo, S.H., Janturan, Warungboto, Umbulharjo, Yogyakarta, 55164, Indonesia

ARTICLE INFO

Keywords:
Sulfate
Nanocarriers
Alkaline phosphatase
Self-emulsifying drug delivery systems
SEDDS
Surfactants
Enzymatic cleavage

ABSTRACT

This study aimed to develop self-emulsifying drug delivery systems (SEDDS) containing sulfate-based surfactants, namely, sodium dodecyl sulfate (SDS), sodium octyl sulfate (SOS) and sodium cetearyl sulfate (SCS), and to evaluate intestinal alkaline phosphatase (IAP)-triggered sulfate release from these SEDDS.

Results showed a time-dependent release of para-nitrophenol from para-nitrophenyl phosphate (p-NPP) and para-nitrophenyl sulfate (p-NPS) when incubated with isolated IAP indicating that the enzyme can also cleave sulfate groups. Moreover, sulfate release from p-NPS and sulfate-based surfactants was observed. SEDDS containing sulfate-based surfactants exhibited a narrow droplet size distribution and polydispersity index (PDI). A droplet size of 35.31 ± 0.41 nm to 41.15 ± 0.98 nm, PDI of 0.17 ± 0.02 to 0.26 ± 0.02 and zeta potential of 9.59 ± 0.85 mV to −18.53 ± 2.75 mV were recorded. Droplet size and PDI showed a minor increase upon contact with isolated IAP. Incubation with isolated IAP caused a rapid sulfate release from sulfate-based surfactant-containing SEDDS (SDS-SEDDS, SOS-SEDDS and SCS-SEDDS). Furthermore, resulting SEDDS exhibited a non-toxic profile. According to these results, SEDDS containing sulfate-based surfactants can be considered as valid alternative to IAP-responsive drug delivery systems containing phosphorylated auxiliary agents.

1. Introduction

Charge-converting nanocarriers hold high potential in the field of nanomedicine [1]. Among these systems, phosphate-decorated nanoparticles (NPs) are of particular interest since phosphate groups are efficiently cleaved by alkaline phosphatase causing a charge conversion from negative to positive. Such systems are of particular interest to overcome the mucus gel layer and to guarantee an efficient uptake by epithelial cells. As the mucus gel layer exhibits an anionic charge because of sialic and sulfonic substructures, anionic nanoparticles can to a high extent permeate this three-dimensional network of mucus glycoproteins [2,3]. Having reached the absorption membrane, the membrane bound enzyme intestinal alkaline phosphatase (IAP) cleaves the phosphate groups on the surface of these nanoparticles causing charge conversion [4–6]. The resulting positive surface charge triggers their cellular uptake as a positive surface charge induces endocytosis [7]. Moreover, the virus-mimicking strategy has been reported to enable nanocarriers to overcome the mucus barrier and to provide a targeted release at the underlying epithelium [4,8]. Likewise, ALP-responsive surface decoration of lipid-based formulations enabled an enhanced cellular uptake following the cleavage of phosphate moieties revealing underlying positive surface charges at the target cell membranes [9,10].

Although phosphorylated surfactants have shown potential for the design of such nanoparticles, none of them is listed in the FDA data base of inactive ingredients [11,12]. The development of pharmaceutical products utilizing this technology is therefore unlikely. An alternative might be sulfate-based surfactants since they are listed in this data base and widely employed by the pharmaceutical industry [13–15]. Furthermore, alkaline phosphatase was shown to cleave not just phosphates but also sulfates [16,17]. In addition, sulfate-based surfactants

* Corresponding author. University of Innsbruck, Institute of Pharmacy, Pharmaceutical Technology, Center for Chemistry and Biomedicine, Innrain 80–82/IV, A-6020, Innsbruck, Austria.
E-mail address: andreas.bernkop@uibk.ac.at (A. Bernkop-Schnürch).

https://doi.org/10.1016/j.jddst.2024.105717
Received 16 January 2024; Received in revised form 10 April 2024; Accepted 24 April 2024
Available online 30 April 2024

are suitable excipients for the formation of stable self-emulsifying drug delivery systems (SEDDS) owing to their amphiphilic properties [18]. So far, however, the potential of sulfate-based surfactants for the design of charge-converting nanoparticles has not been evaluated.

According to our study hypothesis, that sulfate groups can be cleaved from surfactants like phosphate groups, it was the aim of this study to design IAP-responsive SEDDS containing sulfate-based surfactants and to evaluate the potential of such systems *in vitro*. SDS is generally recognized as safe by the Food and Drug Administration [19]. Since various studies have shown that the hydrophobic tail structure has a major impact on the performance of drug delivery systems, hydrophobic tails of different chain length were tested. Sulfate groups can be cleaved from the surface of SEDDS droplets containing sulfate-based surfactants triggered by IAP. Moreover, the commercially available sodium dodecyl sulfate (SDS), sodium octyl sulfate (SOS) and sodium cetearyl sulfate (SCS) can be considered as alternative excipients to phosphorylated surfactants since they can form stable SEDDS and their sulfate groups can be cleaved off by IAP. To that end, SDS, SOS and SCS were incorporated into SEDDS. The resulting nanocarriers were characterised regarding droplet size, polydispersity index (PDI) and zeta potential. IAP-responsive cleavage of sulfate groups from these SEDDS was evaluated by quantifying sulfate release as a function of time. Moreover, cytotoxicity of these SEDDS was investigated on Caco-2 cells.

2. Material and methods

2.1. Materials

4-Nitrophenyl sulfate potassium salt (p-NPS), 4-Nitrophenyl phosphate disodium hexahydrate (p-NPP), sodium octyl sulfate (SOS), Cremophor EL (polyoxyl 35 hydrogenated castor oil), Tween 80 (poly oxyethylene sorbitan monooleate), propylene glycol, oleic acid ethyl ester, triacetin, Triton X-100, alkaline phosphatase from bovine intestinal mucosa (7165 units/mg protein), ammonium molybdate tetrahydrate (81–83 %), glucose-D-(+) ≥ 99.5 % anhydrous, hydrochloric acid, sodium hydroxide, minimum essential medium (MEM), phosphatase inhibitor cocktail-2 (PIC-2) and resazurin sodium salt were purchased from Sigma-Aldrich, Austria. Lanette E (alcohol sulfate mono-C16-18 sodium salt, SCS) was purchased from BASF (St. Augustin, Germany). Sodium dodecyl sulfate (SDS) and 4-(2-hydroxyethyl)-1-piperazineethanesulfonic acid (HEPES) ≥ 99.5 % were obtained from ROTH GmbH (Karlsruhe, Germany). Capmul MCM (caprylic/capric mono and diglycerides) and Captex 355 (glyceryl tricaprylate/caprate) were received from Abitec, USA. Eriochrome® Black T was obtained from Fluka Analytica, Austria. All other chemicals were analytical grade.

2.2. Enzyme-triggered release of sulfate

2.2.1. Para-nitrophenol release from p-NPS and p-NPP by isolated IAP

To investigate the catalytic activity of IAP on sulfate groups, p-NPS and p-NPP were employed as substrates. Accordingly, 5 mg of p-NPS and p-NPP were dissolved in 50 mM HEPES buffer pH 7.2 reaching a final volume of 3 mL. Thereafter, 13 μL of isolated IAP solution (10 U/mL) was added to each mixture and incubated at 37 °C under constant shaking at 350 rpm using a Thermomixer (Eppendorf, Germany). Aliquots of 100 μL from each mixture were transferred to 96 well plates at set time intervals (0, 2, 4 and 24 h) and absorbance of para-nitrophenol was measured at a wavelength of 405 nm using a microplate reader (Tecan Infinite M200; Grödig, Austria). The p-NPS and p-NPP solutions incubated without isolated IAP served as control groups.

To determine also the sulfate release from p-NPS upon cleavage of the sulfate bond, a titrimetric assay was performed based on a previously described method with slight modifications [20]. In brief, 150 mg of p-NPS was dissolved in 6 mL of 50 mM HEPES buffer pH 7.2. Thereafter, 780 μL of 5 U/mL and 10 U/mL of isolated IAP were added to 6 mL of sample solution. Thereafter, all samples were incubated at 37 °C under constant shaking at 350 rpm using a Thermomixer (Eppendorf, Hamburg, Germany). At predetermined time points (0, 2, 4 and 24 h), 1 mL of aliquots was collected and diluted with distilled water up to a total volume of 50 mL. Then, 7.5 mL of 0.05 M $BaCl_2$ was added to this solution under constant stirring for 5 min. Afterwards, 5 mL of buffer solution containing 54 g/L ammonium chloride and 87.5 g/L ammonia was added under constant stirring for 5 min. Thereafter, pH was adjusted to 3.3 with 1 M HCl. Dispersions were filtered through a 0.2 μm pore-sized cellulose acetate membrane (Sartorius AG, Gottingen, Germany). The indicator Eriochrome Black T (EBT) was added to the samples. Titration was performed with 100 mM EDTA until equivalence points. In parallel, the experiment was carried out without substrate under the same conditions serving as blank.

The released sulfate was quantified using the following equation:

$$SO_4^{2-} = \frac{(BLK - Veq) \times C\ EDTA \times MWs}{Sample\ Volume\ (L)} \times 10^3$$

where SO_4^{2-} is sulfate content in mg/L (μg/mL), BLK is volume of barium chloride solution in L, Veq is titrant consumption until the equivalent point in L, C EDTA is concentration of the selected titrant in mol/L (EDTA = 0.05 mol/L), MWs is molecular weight of the sulfate in g/mol (96.063 g/mol).

2.2.2. Para-nitrophenol release from p-NPS by Caco-2 cell-derived IAP

In order to investigate the enzyme-responsive cleavage of sulfate groups from p-NPS forming para-nitrophenol, IAP-expressing Caco-2 cells were utilised. Accordingly, Caco-2 cells were obtained from the European Collection of Authenticated Cell Cultures (ECACC, health protection agency, UK). Cells were seeded in 24-well plates at a density of 25.000 cells/well with MEM supplemented with 10 % of fetal bovine serum (FBS) and 1 % of penicillin-streptomycin at 37 °C in an atmosphere containing 5 % CO_2. The old MEM was changed on alternate days until a cell monolayer was obtained. Before the experiment, cells were washed twice with 500 μL of glucose-HEPES buffer pH 7.4. The control cells were incubated with 500 μL of glucose-HEPES buffer containing 0.1 % and 0.05 % (v/v) phosphatase inhibitor cocktail 1 h before the experiment. Afterwards, cells were washed again and incubated with 500 μL of 50 mg/mL of sulfate solutions in glucose-HEPES buffer. As a control, the experiment was performed under equivalent conditions with samples containing 0.1 and 0.05 % (v/v) phosphatase inhibitor cocktail. Aliquots of 100 μL from each well were transferred to 96 well plates at set time intervals (0, 2, 4 and 24 h) and absorbance of para-nitrophenol was measured at a wavelength of 405 nm using a microplate reader (Tecan Infinite M200; Grödig, Austria).

2.3. Determination of sulfate release from sulfate-based surfactants

In case of sulfate-based surfactants (SDS, SOS and SCS as shown in Table 1), 130 μL of isolated IAP 10 U/mL was added to 5 mL of each compound solution (25 mg/mL in 50 mM HEPES buffer pH 7.2). Thereafter, all samples were incubated at 37 °C under constant shaking at 350 rpm using a Thermomixer (Eppendorf, Hamburg, Germany). At predetermined time points (0, 2, 4 and 24 h) 1 mL of aliquots was collected and diluted with distilled water up to a total volume of 50 mL and released sulfate was quantified as described above.

2.4. Preparation of SEDDS formulations

Blank SEDDS pre-concentrates were prepared using the excipient ratios as listed in Table 2. Blank SEDDS pre-concentrates were prepared by mixing surfactants, co-solvents and oils under constant shaking at 1500 rpm using Thermomixer (Eppendorf, Germany) at 37 °C for 1 h. To prepare SEDDS containing sulfate-based compounds, 1 % (m/v) of SDS, SOS, and SCS were added to blank SEDDS, respectively.

Table 1
Chemical structure of sulfate compounds incorporated in SEDDS.

Chemical name	Chain length	Molecular weight (g/mol)	Structure
Sodium dodecyl sulfate (SDS)	C-12	288.38	
Sodium octyl sulfate (SOS)	C8	232.27	
Sodium cetearyl Sulfate (SCS)	C16-18	694	

Table 2
Composition of blank SEDDS and amounts of ingredients as % (v/v).

Formulations	Cremophor EL	Capmul MCM	Captex 355	Propylene glycol	Tween 80	Ethyl Oleat	Glycerol 85	Triacetin	Olive oil
F1		20	20		50		10		
F2					50	30	10	10	
F3	30	30	30	10					
F4					50		10		40

2.5. Characterizing the surface modifications of SEDDS formulations

To determine the surface modification from all SEDDS formulations, SDS-SEDDS, SOS-SEDDS and SCS-SEDDS were characterized based on a previously established method with slight modifications [3,21]. Accordingly, all SEDDS pre-concentrates were emulsified 1:1000 (v/v) in 20 mM HEPES buffer pH 7.4. All SEDDS formulations were then formed and further mixed for 2 min under constant shaking at 350 rpm using Thermomixer (Eppendorf, Germany) at 37 °C before characterization. Thereafter, all formulations were evaluated regarding mean droplet size, PDI and zeta potential using Zetasizer Nano ZSP under an angle of 90° (Malvern Instruments, Worcestershire, UK). Triplicated evaluations were carried out at 25 °C.

2.6. Cytotoxicity studies

To evaluate potential cytotoxicity of SEDDS containing sulfate compounds, resazurin assay was utilised on Caco-2 cells based on a previously described method with minor modifications [3,22]. Before the experiment, Caco-2 cells were cultivated as described above and washed twice with glucose–HEPES. Thereafter, SEDDS were diluted with glucose-HEPES buffer in ratios of 1:1000, 1:500 and 1:250 v/v and 500 μL of these diluted formulations were transferred to the well plates containing Caco-2 cells following an incubation at 37 °C for 6 and 24 h. Glucose – HEPES buffer pH 7.4 was utilised as negative control and 0.5 % (m/v) Triton X-100 solution in glucose–HEPES buffer served as positive control. At predetermined time points, cells were washed twice with 500 μL of the pre-warmed glucose–HEPES buffer. Afterwards, 250 μL of 2.2 mM resazurin solution was added to each well and incubated at 37 °C in dark conditions for 3 h. Then, 100 μL of aliquots from each well were transferred to a 96-well black plate and fluorescent intensity was measured at an excitation wavelength (λex) of 540 nm and an emission wavelength (λem) of 590 nm using a microplate reader (Tecan Infinite M200; Grödig, Austria). Cell viability was evaluated using the following equation:

$$\%\ \text{Cell viability} = \frac{\text{Sample fluorescence}}{\text{negative control fluorescence}} \times 100$$

2.7. Enzyme-induced changes in droplet size and zeta potential

In order to evaluate the destabilisation of SEDDS containing SDS, SOS and SCS isolated IAP was added to formulations. In detail, each SEDDS formulation was diluted 1:500 (v/v) in 5 mL of 20 mM HEPES pH 7.4 and 10 U/mL isolated IAP was added to this dilution. Afterwards, these samples were incubated at 37 °C under constant shaking at 350 rpm using a Thermomixer (Eppendorf, Germany). At predetermined time points, (0, 1, 2, 3 and 6 h), aliquots of 100 μL were collected and analysed regarding droplet size, PDI and zeta potential using a Zetasizer Nano ZS (Malvern Instruments, UK). Triplicated evaluations were carried out at 25 °C with a detection angle of 173°.

2.8. Sulfate cleavage from SEDDS by isolated IAP

In order to investigate the sulfate cleavage from SEDDS containing SDS, SOS and SCS, isolated IAP was utilised. In detail, SEDDS containing SDS, SOS and SCS were diluted 1: 500 (v/v) in 5 mL of 20 mM HEPES pH 7.4 buffer and 86.4 μL of isolated IAP (10 U/mL) was added to this solution. Then, samples were incubated under constant shaking at 350 rpm using Thermomixer (Eppendorf, Germany) at 37 °C. At predetermined time points (0, 2, 4 and 24 h) aliquots of 1 mL were collected and diluted with distilled water up to a total volume of 50 mL. Samples omitting isolated IAP served as control. Time-dependent sulfate release from SEDDS containing SDS, SOS and SCS was evaluated as described in section 2.3.

2.9. Statistical data analysis

The statistical analysis of data was performed by Graph Pad Prism 5.01 software. Mean ± standard deviation (SD) of the results were based on at least three experiments. Unpaired student's t-test was employed to analyse the differences between two independent groups. The level of significance was set as significant (*$p < 0.05$), very significant (**$p < 0.01$) and highly significant (***$p < 0.005$).

3. Results and discussion

3.1. IAP-responsive sulfate cleavage from p-NPS

Phosphatase-responsive prodrugs and drug delivery systems enable a targeted drug release employing this membrane bound enzyme of eukaryotic cells that can cleave phosphate groups from a variety of substrates [23–27]. p-NPP is utilised as well-established substrate of IAP for the development of such enzyme-responsive DDS [28]. In order to confirm these results the time-dependent formation of para-nitrophenol from p-NPS upon cleavage of sulfate bonds following IAP treatment was

investigated. Results are shown in Fig. 1 p-NPP was used as positive control to confirm enzymatic activity of IAP under the studied conditions.

As shown in Fig. 1, within 24 h the absorbance of released para-nitrophenol from p-NPP was 12.6-fold higher than that from p-NPS, whereas without the addition of IAP there was no significant difference in the increase in absorbance of these two substrates ($p \geq 0.001$, Student's t-test). These results indicate that absorbance of para-nitrophenol increased in a time-dependent manner due to the cleavage of both phosphate and sulfate groups from the substrates. Moreover, similar to results obtained with p-NPP, a significantly higher absorbance increase was observed when p-NPS was incubated with IAP compared with the control group omitting IAP indicating that sulfate cleavage was also IAP-dependent like phosphate cleavage. Since IAP is to a minor extent also released from the cellular membrane cleaving anionic substructures on the surface of nanocarriers already on their way to the absorptive membrane, a too rapid cleavage might be disadvantageous [24,29]. As a proof of concept study, we evaluated the ALP-responsiveness of SEDDS-containing surface sulfate groups using commercially available sulfate-based surfactants namely SOS, SDS and SCS. Other sulfate-containing surfactants, however, might exhibit higher ALP-responsiveness. Generally, these experiments demonstrated that both p-NPS and p-NPP are accessible for isolated IAP. The chemical mechanism of sulfate cleavage is illustrate in Fig. 2.

This result was in good agreement with a previous study carried out by Andrews et al. demonstrating that alkaline phosphatase can catalyse the hydrolysis of p-NPS releasing sulfate [16]. Nikolic-Hughes et al. confirmed also the cleavage of sulfate groups from p-NPS by alkaline phosphatase [30].

Furthermore, sulfate release from p-NPS was monitored using two different concentrations of isolated IAP under physiological conditions. The results are shown in Fig. 3.

As illustrated in Fig. 3, within 24 h approximately 16.29 % of sulfate was released from p-NPS, when the substrate was incubated with 10 U/mL of isolated IAP. In case of 5 U/mL of IAP addition only 7.72 % of sulfate was released within 24 h. Moreover, negligible amounts of sulfate were released from the substrate in the absence of isolated IAP. These results indicate that the extent of sulfate release correlates with increasing concentrations of isolated IAP cleaving sulfate bonds from p-NPS. Similarly, Hock et al. reported a concentration-dependent catalytic activity of isolated IAP when incubated with amikacin-loaded polyphosphate nanoparticles under physiological conditions [31].

3.1.1. Para-nitrophenol release from p-NPS by Caco-2 cell-derived IAP

To confirm that membrane-bound IAP can also cleave sulfate from p-NPS, Caco 2-cells were utilised which express IAP resembling the human intestinal brush border membrane [32–34]. Results of this study are shown in Fig. 4.

As shown in Fig. 4, a significantly increased absorbance was observed within 24 h of incubation as a result of sulfate release ($p \leq 0.001$, Student's t-test). In contrast, only a negligible amount of para-nitrophenol was released in the presence of an inhibitor cocktail (PIC-2). The observation is in accordance with previous studies, showing that the activity of IAP on Caco-2 cells is lower in presence of PIC-2 [35]. According to these results, p-NPS is also accessible for membrane-bound IAP.

3.2. Enzymatic sulfate cleavage from sulfate-based surfactants

Within this study the sulfate-based surfactants SDS, SOS and SCS were incorporated into SEDDS.SDS is a sulfate ester of lauryl alcohol (C12) and mostly used for the development DDS [36,37]. SOS as an alkyl sulfate has a shorter chain length (C8) linked to a polar sulfate group [38]. SCS another alkyl sulfate consisting of a long carbon chain (C16-18) which has also been utilised for the development of lipid based nanocarriers [39]. The amphipathic properties of sulfate compounds make them suitable for incorporation into SEDDS. In order to confirm IAP-triggered sulfate release from these compounds, they were incubated with isolated IAP. Results of the resulting sulfate release are shown in Fig. 5.

As illustrated in Fig. 5, within the first 24 h approximately 23.1 %, 16.4 % and 6.96 % of sulfate was released from SDS, SOS and SCS, respectively. However, after 4 h lower release of sulfate was observed in the presence of isolated IAP. At the end of the experiment, the amount of released sulfate followed the rank order: SDS > SOS > SCS. These results were in accordance with the catalytic activity of IAP as shown in Fig. 3. Moreover, the lipophilic chain length of the surfactant plays a key role in sulfate release from SEDDS. Since concentrations of 1 % (m/v) sulfate-based surfactants in each formulation and the number of sulfate groups in the surfactant molecule are the same, lipophilic chain length might have an effect on the IAP-responsive sulfate release from SEDDS. Surfactants with longer lipophilic chains exhibited lower sulfate release from the surface of SEDDS that can be explained by a more efficient incorporation of such surfactants into the oily droplet core due to their longer lipophilic moiety limiting the contact of IAP with surface sulfate groups.

3.3. Preparations and characterization of SEDDS

Blank SEDDS formulations were investigated regarding their size, PDI and zeta potential as shown in Table 3.

Since formulation F3 exhibited a narrow droplet size of 35.70 ± 0.62 nm, PDI of 0.08 ± 0.02 indicating a more homogeneous dispersion and a zeta potential of −13.70 ± 2.98 mV, it was chosen for further studies. Moreover, F3 contains Cremophor EL, a surfactant providing PEGylation on the nanodroplet surface. The presence of PEG chains on the surface of the nanocarrier prevents digestive enzymes to access and degrade the lipid content of the nanocarrier [40]. In addition, the stability of the lipid content in the nanocarrier is also determined by the length of the fatty acid chain and the degree of glycerol esterification. Long fatty acid

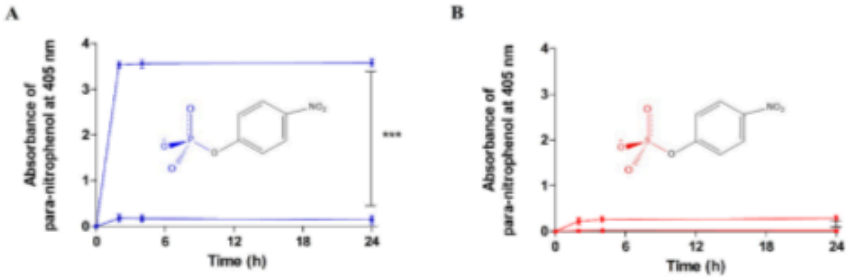

Fig. 1. Time-dependent absorbance increase of para-nitrophenol upon hydrolysis of (A) p-NPP as positive control and (B) p-NPS. Samples were incubated with (blue and red circles) and without (blue and red squares) isolated IAP at 37 °C, respectively. Data are indicated as means ± SD (n = 3). (*** = $p \leq 0.001$). (For interpretation of the references to colour in this figure legend, the reader is referred to the Web version of this article.)

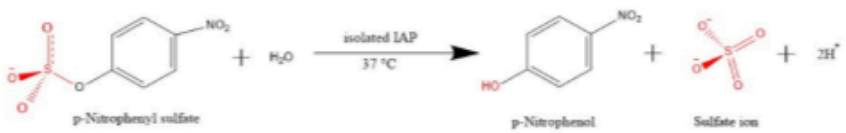

Fig. 2. Schematic illustration of cleavage of sulfate groups by IAP releasing p-nitrophenol.

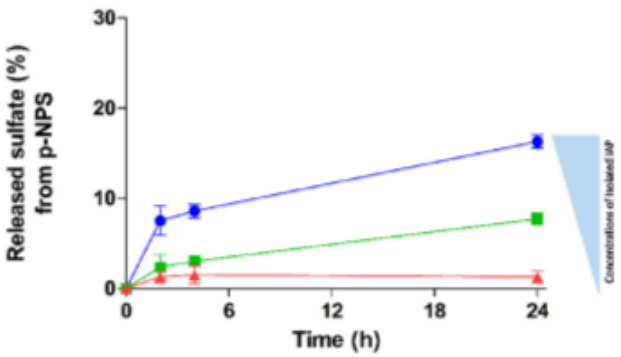

Fig. 3. Released sulfate from p-NPS incubated with isolated 10 U/mL (blue circles) and 5 U/mL (green squares) of IAP and without IAP (red triangles). Evaluations were made at 37 °C by triple titration using 0.1 M EDTA as titrant and EBT as indicator. Data are shown as means ± SD (n = 3). (For interpretation of the references to colour in this figure legend, the reader is referred to the Web version of this article.)

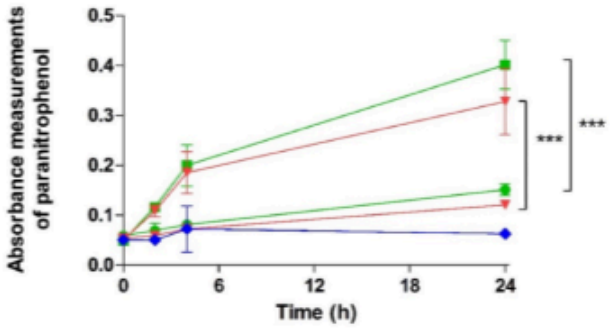

Fig. 4. Time-dependent increase in absorbance of para-nitrophenol formed by release of sulfate groups from p-NPS by Caco-2 cell-derived IAP. Green squares and green circles represent the absorbance of p-NPS incubated by absence and presence of PIC-2 (0.1 %v/v), while orange triangles and reverse triangles represent absorbance of p-NPS incubated by absence and presence of PIC-2 (0.05 %v/v) and the blue triangles represent glucose HEPES buffer. Data are indicated as means ± SD (n = 3). (*** = $p \leq 0.001$). (For interpretation of the references to colour in this figure legend, the reader is referred to the Web version of this article.)

chains show higher stability than short and medium chains. Regarding the degree of glycerol esterification, mono- and di-glycerides are more easily degraded by lipase than triglycerides [40,41]. Moreover, long chain fatty acids and high levels of esterification tend to cause larger droplets. In this study, medium chain triglycerides (Captex 355) were selected and combined with mono- and di-glycerides (Capmul MCM) to obtain small droplet sizes. Apart from functioning as solvents, mono- and di-glycerides also act as lipophilic surfactants which provide a beneficial effect in reducing droplet size. Accordingly, 1 % (m/v) of SDS, SOS and SCS were incorporated into formulation F3 and characterised as displayed in Table 4.

As illustrated in Table 4, all SEDDS exhibited a small size (≤50 nm) with a PDI ranging from 0.17 ± 0.02 to 0.26 ± 0.02. Since the PDI of all formulations was ≤0.3, a narrow droplet size distribution was provided. Zeta potential of the formulations followed the rank order: SOS-SEDDS < SDS-SEDDS < SCS-SEDDS. These results might be explained by the combination of caprylic/capric mono- and diglycerides used for F1 and F3 to obtain a smaller droplet size. Furthermore, Leichner et al. reported that by the addition of polyoxyl 35 hydrogenated castor oil, SEDDS show sufficient self-emulsifying properties due to the high HLB value of this surfactant [42]. Moreover, another study showed that polar lipids with a shorter carbon chain enable formation of SEDDS with a smaller droplet size [22,43,44].

3.4. Cytotoxicity of SEDDS

The cytotoxic potential of SDS-SEDDS, SOS-SEDDS and SCS-SEDDS on Caco-2 cells was evaluated by resazurin assay [45,46] and results are shown in Fig. 6. This assay enables assessment of viable cells owing to reduction of resazurin to its highly fluorescent analogue resorufin by alive cells [47,48].

As depicted in Fig. 6, Caco-2 cells well tolerated all formulations in all studied concentrations displaying ≥85 % viability after 6 h. As reported previously [49], compounds leading to ≥ 85 % of cell viability can be regarded as not toxic. However, all formulations exhibited a cell viability ≤80 % after 24 h and a concentration-dependent decrease in cell viability was observed. In general, the highest cytotoxic potential was recorded in case of SCS-SEDDS followed by SDS-SEDDS and SOS-SEDDS. These results are in agreement with other studies where authors reported a tolerability of SEDDS containing polyoxyl 35 hydrogenated castor oil by Caco-2 cells *in vitro* [50–52].

3.5. Enzyme-induced changes in droplet size and zeta potential

Enzyme-induced changes in droplet size, PDI and zeta potential on SDS-SEDDS, SOS-SEDDS and SCS-SEDDS were investigated using isolated IAP. The results are shown are in Fig. 7.

As depicted in Fig. 7, not all formulations remained stable when incubated with IAP as increases in their droplet size and PDI were observed over time. Nevertheless, all formulations still exhibited a narrow droplet size distribution between 34.84 ± 0.95 nm to 96.65 ± 1.05 nm. In detail, after 6 h SDS-SEDDS, SOS-SEDDS and SCS-SEDDS displayed Δ13.6, Δ17.15 and Δ0.18 nm total changes in droplet size, respectively. PDI also increased to ≥0.3 after 3 and 6 h for SDS-SEDDS and SOS-SEDDS, while only SCS-SEDDS exhibited a PDI of ≤0.3. Overall, among the three SEDDS containing sulfate-based surfactants, SEDDS-SCS was sufficiently stable exhibiting minor changes in droplet size and PDI over time. These results revealed that when incubated with isolated IAP droplet size and PDI of SEDDS change depending on the carbon chain length of the sulfate compounds. These results were also in line with the findings of Akkus et al. where the authors utilised various phosphorylated surfactants to form suitable SEDDS resulting also in slight changes in droplet size and PDI when incubated with IAP for 6 h [22]. Moreover, Le-Vinh et al. reported about an increasing size and PDI of solid lipid nanoparticles (SLNs) upon contact with isolated IAP in a time-dependent manner [53]. Apart from size and PDI, an enzyme-triggered shift in zeta potential might have also occurred by incubating SEDDS with isolated IAP. However, within 6 h, no significant

difference in the zeta potential of SEDDS was observed (data not shown). These results might be derived from SEDDS surfaces limiting their entire exposure to isolated IAP and resulting in an insufficient cleavage of sulfate moieties during the studied time period.

3.6. Sulfate cleavage from SEDDS by isolated IAP

In order to confirm cleavage of sulfate moieties from the surface of SDS-SEDDS, SOS-SEDDS and SCS-SEDDS, time-dependent sulfate release was investigated upon incubation with isolated IAP. The results are shown in Fig. 8.

As displayed in Fig. 8, a considerable amount of sulfate was released from all SEDDS in the presence of isolated IAP. Within 6 h, approximately 42.9 %, 38.4 % and 15.3 % of sulfate were release from SDS-SEDDS, SOS-SEDDS and SCS-SEDDS, respectively. In contrast, only negligible amounts of sulfate were released from SEDDS incubated without isolated IAP. The results are in a good agreement with sulfate release data from p-NPS and sulfate-based compounds upon their incubation with isolated IAP as shown in Figs. 3 and 5, respectively. Sulfate release from SCS-SEDDS was slightly lower compared to SOS-SEDDS and SDS-SEDDS. This outcome might be explained by the comparatively longer carbon chain of SCS being to a higher extent embedded in the oily core of SEDDS droplets.

4. Conclusions

In this study, IAP-responsive sulfate release from a lipid-based drug delivery system was shown for the first time providing a proof of concept for an IAP-based activation of such systems containing sulfate-based surfactants. Various sulfate-based surfactants namely, SDS, SOS and SCS were found to form stable SEDDS with a small droplet size displaying a low polydispersity. Moreover, the resulting SEDDS remained

Fig. 5. Sulfate release from SDS (blue circles), SOS (pink squares) and SCS (green triangles) when incubated with IAP at 37 C quantified by triple titration using 0.1
M EDTA as titrant and EBT as indicator. Data are shown as means ± SD (n = 3). (For interpretation of the references to colour in this figure legend, the reader is
referred to the Web version of this article.)

Table 3
Mean droplet size, PDI and zeta potential of blank SEDDS. Diluted 1:500 in 20 mM Hepes buffer pH 7.4. Incubated for 1 h at 37 C. All values are means of n 3 ± SD.

Formulations	Size (nm)	PDI	Zeta potential (mV)
F1	47.99 ± 1.95	0.40 ± 0.00	18.20 ± 1.22
F2	28.69 ± 0.89	0.39 ± 0.01	15.03 ± 0.73
F3	35.70 ± 0.62	0.08 ± 0.02	13.70 ± 2.98
F4	148.97 ± 2.90	0.51 ± 0.00	9.29 ± 0.60

Table 4

Mean droplet size, PDI and zeta potential of 1 % sulfate-based surfactant containing SEDDS diluted 1:500 (v/v) in 20 mM HEPES buffer pH 7.4. All values are means of n 3 ± SD.

Formulations	Size (nm)	PDI	Zeta potential (mV)
SDS-SEDDS	41.15 ± 0.98	0.25 ± 0.00	12.20 ± 0.28
SOS-SEDDS	35.31 ± 0.41	0.17 ± 0.02	9.59 ± 0.85
SCS-SEDDS	39.62 ± 1.82	0.26 ± 0.02	18.53 ± 2.75

Fig. 6. Cell viability of Caco-2 cells incubated with indicated SEDDS. Dark-coloured bars and light-coloured bars depict percentage of cell viability after incubation for 6 and 24 h, respectively. Data are indicated as means ± SD (n = 3).

A. Saleh et al.

sufficiently stable upon incubation with isolated IAP exhibiting minor changes in droplet size following the enzymatic treatment. These SEDDS exhibited a concentration- and time-dependent cytotoxicity on Caco-2 cells. IAP-dependent sulfate release from SEDDS was demonstrated by monitoring the time-dependent sulfate release from the formulations using a titrimetric assay. According to the findings of this study, replacing phosphorylated surfactants with their well-established sulfate-based counterparts might be a promising approach for the development of IAP-responsive lipid-based drug delivery systems. Furthermore, such sulfate surfaces can be utilised in the future for the surface modifications of a broad range of nanocarrier systems as an alternative to phosphate-based surface decorations.

CRediT authorship contribution statement

Ahmad Saleh: Writing – review & editing, Writing – original draft, Methodology, Investigation, Formal analysis, Data curation, Conceptualization. Zeynep Burcu Akkus-Dagdeviren: Writing – review & editing, Methodology, Investigation, Data curation. Florina Veider: Methodology, Investigation. Nuri Ari Efiana: Methodology, Investigation. Andreas Bernkop-Schnürch: Writing – review & editing, Writing – original draft, Supervision, Resources, Methodology, Funding acquisition, Conceptualization.

Declaration of competing interest

The authors declare that they have no known competing financial interests or personal relationships that could have appeared to influence the work reported in this paper.

Data availability

Data will be made available on request.

Fig. 7. Droplet size (A) and PDI (B) of SDS-SEDDS (blue), SOS-SEDDS (pink) and SCS-SEDDS (green) diluted 1:500 in 20 mM HEPES buffer pH 7.4 and incubated with IAP (10 U/mL) at 37 C. Data are shown as means ± SD (n = 3). (For interpretation of the references to colour in this figure legend, the reader is referred to the Web version of this article.)

Fig. 8. Time-dependent sulfate release from SDS-SEDDS (A), SCS-SEDDS (B) and SOS-SEDDS (C). Samples were incubated with (circles) or without (squares) isolated IAP (10 U/mL) at 37 C. Time-dependent sulfate release was quantified by triple titration using 100 mM EDTA as titrant and EBT as indicator. Data are shown as means ± SD (n = 3).

Acknowledgements

The authors would like to greatly acknowledge to the support from The Ministry of Education, Culture, Research and Technology of the Republic of Indonesia for providing the BPPLN scholarship scheme. The authors thank Astrid Bernkop-Schnürch from Green River Polymers Forschungs-und Entwicklungs GmbH for providing materials.

Appendix A. Supplementary data

Supplementary data to this article can be found online at https://doi.org/10.1016/j.jddst.2024.105717.

References

[1] F. Veider, E. Sanchez Armengol, A. Bernkop-Schnürch, Charge-reversible nanoparticles: advanced delivery systems for therapy and diagnosis, Small (2023) 2304713.
[2] A. Bernkop-Schnürch, Strategies to overcome the polycation dilemma in drug delivery, Adv. Drug Deliv. Rev. 136 (2018) 62–72.
[3] W. Suchaoin, et al., Development and in vitro evaluation of zeta potential changing self-emulsifying drug delivery systems for enhanced mucus permeation, Int. J. Pharm. 510 (1) (2016) 255–262.
[4] A. Saleh, et al., Chitosan–Polyphosphate nanoparticles for a targeted drug release at the absorption membrane, Heliyon 8 (9) (2022) e10577.
[5] B. Le-Vinh, et al., Alkaline phosphatase: a reliable endogenous partner for drug delivery and diagnostics, Advanced Therapeutics (2022) 2100219.
[6] H. Spleis, et al., Surface design of nanocarriers: key to more efficient oral drug delivery systems, Adv. Colloid Interface Sci. (2023) 102848.
[7] S. Haddadzadegan, F. Dorkoosh, A. Bernkop-Schnürch, Oral delivery of therapeutic peptides and proteins: technology landscape of lipid-based nanocarriers, Adv. Drug Deliv. Rev. 182 (2022) 114097.
[8] S. Dünnhaupt, et al., Nano-carrier systems: strategies to overcome the mucus gel barrier, Eur. J. Pharm. Biopharm. 96 (2015) 447–453.
[9] P. Knoll, et al., Charge converting nanostructured lipid carriers containing a cell-penetrating peptide for enhanced cellular uptake, J. Colloid Interface Sci. 628 (2022) 463–475.
[10] F. Veider, et al., Overcoming intestinal barriers by heparanase-responsive charge-converting nanocarriers, Int. J. Pharm. (2024) 123817.
[11] T.V. Kulakovskaya, V.M. Vagabov, I.S. Kulaev, Inorganic polyphosphate in industry, agriculture and medicine: modern state and outlook, Process Biochem. 47 (1) (2012) 1–10.
[12] Z.B. Akkus, et al., Zeta potential changing polyphosphate nanoparticles: a promising approach to overcome the mucus and epithelial barrier, Mol. Pharm. 16 (6) (2019) 2817–2825.
[13] M.J. Lawrence, Surfactant systems: microemulsions and vesicles as vehicles for drug delivery, Eur. J. Drug Metabol. Pharmacokinet. 19 (3) (1994) 257–269.
[14] D.E. Riechers, et al., Surfactant effects on glyphosate efficacy, Weed Technol. 9 (2) (1995) 281–285.
[15] C. Reich, C.R. Robbins, surfaces: light-scattering and radiotracer studies, J. Soc. Cosmet. Chem. 44 (1993) 263–278.
[16] L.D. Andrews, J.G. Zalatan, D. Herschlag, Probing the origins of catalytic discrimination between phosphate and sulfate monoester hydrolysis: comparative analysis of alkaline phosphatase and protein tyrosine phosphatases, Biochemistry 53 (43) (2014) 6811–6819.
[17] P.J. O'Brie, D. Herschlag, Functional interrelationships in the alkaline phosphatase superfamily: phosphodiesterase activity of Escherichia coli alkaline phosphatase, Biochemistry 40 (19) (2001) 5691–5699.
[18] T. Cserháti, E. Forgács, G. Oros, Biological activity and environmental impact of anionic surfactants, Environ. Int. 28 (5) (2002) 337–348.
[19] M. Zhou, M.P. Doyle, D. Chen, Combination of levulinic acid and sodium dodecyl sulfate on inactivation of foodborne microorganisms: a review, Crit. Rev. Food Sci. Nutr. 60 (15) (2020) 2526–2531.
[20] J.S. Fritz, M. Freeland, Direct titrimetric determination of sulfate, Anal. Chem. 26 (10) (1954) 1593–1595.
[21] J.G. Nørby, M. Esmann, The effect of ionic strength and specific anions on substrate binding and hydrolytic activities of Na, K-ATPase, J. Gen. Physiol. 109 (5) (1997) 555–570.
[22] Z.B. Akkuş-Dağdeviren, et al., Charge reversal self-emulsifying drug delivery systems: a comparative study among various phosphorylated surfactants, J. Colloid Interface Sci. 589 (2021) 532–544.
[23] R.B. McComb, G.N. Bowers Jr., S. Posen, Alkaline Phosphatase, Springer Science & Business Media, 2013.
[24] A. Saleh, et al., Peptide antibiotic–polyphosphate nanoparticles: a promising strategy to overcome the enzymatic and mucus barrier of the intestine, Biomacromolecules 24 (6) (2023) 2587–2595.
[25] Z.B. Akkuş-Dağdeviren, et al., Phosphatase-degradable nanoparticles: a game-changing approach for the delivery of antifungal proteins, J. Colloid Interface Sci. 646 (2023) 290–300.
[26] M. Sugiura, et al., Purification of human intestinal alkaline phosphatase, Chem. Pharm. Bull. 23 (7) (1975) 1537–1541.
[27] H. Akcakaya, A. Aroymak, S. Gokce, A quantitative colorimetric method of measuring alkaline phosphatase activity in eukaryotic cell membranes, Cell Biol. Int. 31 (2) (2007) 186–190.
[28] J. Griesser, et al., Highly mucus permeating and zeta potential changing self-emulsifying drug delivery systems: a potent gene delivery model for causal treatment of cystic fibrosis, Int. J. Pharm. 557 (2019) 124–134.
[29] C. Leichner, et al., Intestinal enzyme delivery: chitosan/tripolyphosphate nanoparticles providing a targeted release behind the mucus gel barrier, Eur. J. Pharm. Biopharm. 144 (2019) 125–131.
[30] I. Nikolic-Hughes, P.J. O'brien, D. Herschlag, Alkaline phosphatase catalysis is ultrasensitive to charge sequestered between the active site zinc ions, J. Am. Chem. Soc. 127 (26) (2005) 9314–9315.
[31] N. Hock, et al., Design of biodegradable nanoparticles for enzyme-controlled long-acting drug release, J. Drug Deliv. Sci. Technol. (2023) 105085.
[32] H. Yuan, N. Li, Y. Lai, Evaluation of in vitro models for screening alkaline phosphatase-mediated bioconversion of phosphate ester prodrugs, Drug Metabol. Dispos. 37 (7) (2009) 1443–1447.
[33] J. Keemink, C.A. Bergström, Caco-2 cell conditions enabling studies of drug absorption from digestible lipid-based formulations, Pharmaceut. Res. 35 (2018) 1–11.
[34] F. Veider, et al., Design of nanostructured lipid carriers and solid lipid nanoparticles for enhanced cellular uptake, Int. J. Pharm. 624 (2022) 122014.
[35] I. Nazir, et al., Zeta potential changing self-emulsifying drug delivery systems: a promising strategy to sequentially overcome mucus and epithelial barrier, Eur. J. Pharm. Biopharm. 144 (2019) 40–49.
[36] N.S. Madhav, et al., Orotransmucosal drug delivery systems: a review, J. Contr. Release 140 (1) (2009) 2–11.
[37] T.P. Niraula, et al., Sodium dodecylsulphate: a very useful surfactant for scientific investigations, J. Knowl. Innov 2 (2014) 111–113.
[38] A. Wibbertmann, et al., Toxicological properties and risk assessment of the anionic surfactants category: alkyl sulfates, primary alkane sulfonates, and α-olefin sulfonates, Ecotoxicol. Environ. Saf. 74 (5) (2011) 1089–1106.
[39] M.S. Khan, et al., Potential of lipid-based nanocarriers against two major barriers to drug delivery—skin and blood–brain barrier, Membranes 13 (3) (2023) 343.
[40] K. Zöller, et al., Digestion of lipid excipients and lipid-based nanocarriers by pancreatic lipase and pancreatin, Eur. J. Pharm. Biopharm. 176 (2022) 32–42.
[41] P. Benito-Gallo, et al., Chain length affects pancreatic lipase activity and the extent and pH–time profile of triglyceride lipolysis, Eur. J. Pharm. Biopharm. 93 (2015) 353–362.
[42] C. Leichner, et al., Development and in vitro characterization of a papain loaded mucolytic self-emulsifying drug delivery system (SEDDS), Int. J. Pharm. 530 (1–2) (2017) 346–353.
[43] B. Singh, et al., Self-nanoemulsifying systems for oral bioavailability enhancement: recent paradigms, in: Fabrication and Self-Assembly of Nanobiomaterials, Elsevier, 2016, pp. 91–115.
[44] V.T. Bhalani, S.P. Patel, Pharmaceutical Compositions for Lipophilic Drugs, Google Patents, 2006.
[45] S. Ferruzza, et al., A protocol for differentiation of human intestinal Caco-2 cells in asymmetric serum-containing medium, Toxicol. Vitro 26 (8) (2012) 1252–1255.
[46] I. Shahzadi, et al., Nanostructured lipid carriers (NLCs) for oral peptide drug delivery: about the impact of surface decoration, Pharmaceutics 13 (8) (2021) 1312.
[47] F. Veider, et al., Design of nanostructured lipid carriers and solid lipid nanoparticles for enhanced cellular uptake, Int. J. Pharm. 624 (2022) 122014.
[48] R. Csepregi, et al., Complex formation of resorufin and resazurin with B-cyclodextrins: can cyclodextrins interfere with a resazurin cell viability assay? Molecules 23 (2) (2018) 382.
[49] J. López-García, et al., HaCaT keratinocytes response on antimicrobial atelocollagen substrates: extent of cytotoxicity, cell viability and proliferation, J. Funct. Biomater. 5 (2) (2014) 43–57.
[50] S. Hauptstein, F. Prüfert, A. Bernkop-Schnürch, Self-nanoemulsifying drug delivery systems as novel approach for pDNA drug delivery, Int. J. Pharm. 487 (1–2) (2015) 25–31.
[51] H.H. Desai, et al., Evaluation of cytotoxicity of self-emulsifying formulations containing long-chain lipids using Caco-2 cell model: superior safety profile compared to medium-chain lipids, J. Pharmaceut. Sci. 109 (5) (2020) 1752–1764.
[52] M.A. Rahman, et al., Role of excipients in successful development of self-emulsifying/microemulsifying drug delivery system (SEDDS/SMEDDS), Drug Dev. Ind. Pharm. 39 (1) (2013) 1–19.
[53] B. Le-Vinh, et al., Size shifting of solid lipid nanoparticle system triggered by alkaline phosphatase for site specific mucosal drug delivery, Eur. J. Pharm. Biopharm. 163 (2021) 109–119.